RSC Advances




ROYAL SOCIETY OF CHEMISTRY

www.rsc.org/advances

A table of contents entry

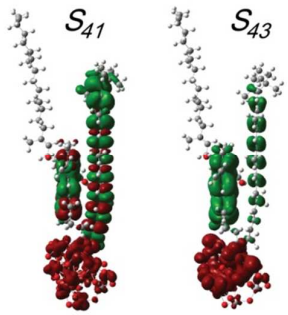


The photoinduced electron transfer, energy transfer and photoelectric conversion efficiency for Bioorganic dye-sensitized solar cell of carotenoid-pheophytin *a*-$TiO_2$ have been systematically investigated

Cite this: DOI: 10.1039/c0xx00000x

www.rsc.org/xxxxxx

ARTICLE TYPE

# Bioorganic dye-sensitized solar cell of carotenoid-pheophytin *a*-$TiO_2$

**Yanting Feng,[a,b,#] Lingyan Meng,[b,#] Jinfeng Zhao,[a,c] Yongqing Li,[*,a,c] Mengtao Sun,[*,b] Jianing Chen[*,b]**

***Received (in XXX, XXX) Xth XXXXXXXXX 20XX, Accepted Xth XXXXXXXXX 20XX***

The isolated carotenoid and pheophytin *a*, the complex of carotenoid-pheophytin *a* and carotenoid-pheophytin *a*-$TiO_2$ film have been investigated, using time-dependent density functional theory. Charge transfer mechanisms have been revealed by the three-dimensional visualization technology. The photoinduced electron transfer, energy transfer and photoelectric conversion efficiency have been systematically investigated in above systems. Furthermore, the charge transfer mechanism and the energy transfer mechanism have been studied when the investigated systems were optically excited in electronic transitions.

## Introduction

Benefiting from advantages of low cost of fabrication,[1] physical flexibility, suitable mass production and less damage to the environment,[2-5] the organic solar cells are supposed to be a potential technology for next generation clear energy. Compared to the inorganic silicon solar cells, the great superiorities make the organic solar cells possess a huge development prospect. The organic solar cells are mainly used to realize the photovoltaic conversion based on the semiconductors as the active material. In the past few years, theoretical and experimental investigations have been mainly focused on finding novel and low-cost ways to transfer the solar radiation to electric energy. The photoelectric conversions of various semiconductor electrodes and electrolyte systems have been widely studied.[6-8] Since 1990s, nanoscale semiconductor organic composite materials have turned to be the main research object of photoelectric conversion, due to the appearance and rapid development of the novel active materials. Unfortunately, the organic solar cell has not been widely adopted in people's lives, because of low photoelectric conversion efficiency, narrow spectral response range and instability of cell performance.[9-11] In recent years, despite the organic solar cells have experienced rapid developments, they still remain in developing stages and thus lots of questions on science and technology still need to be performed and improved.[12]

Dye-sensitized solar cell (DSSC) has a number of attractive features; it is simple to make using conventional roll-printing techniques, is semi-flexible and semi-transparent which offers a variety of uses not applicable to glass-based systems, and most of the materials used are low-cost.[13] For bioorganic system, no pollution occurred after cell destructed, and low-cost make them better active materials for the organic solar cell. In photosynthesis, the role of most pheophytin *a* is to absorb and transfer the solar radiation. Because of the structural characteristics of the porphyrin, the pheophytin *a* has a long life of excited states that can ensure the effective charge separation. Due to the special π system in the porphyrin molecule, the pheophytin *a* can introduce some functional groups into the molecule system, which can broaden the spectrum response range and then improve the photoelectric conversion efficiency. The spectral response of the carotenoid is particularly important to external solar radiation because the carotenoid serves as the electron donor to absorb photons in the carotenoid-pheophytin *a* molecule system. However, the spectral response of carotenoid is around 400 nm, which can directly affect the photoelectric conversion efficiency. Wu and co-workers have found that red-shift phenomenon of the absorption of S band can be induced while introducing the electronic group into the middle position of the porphyrin, which lowers the HOMO-LUMO energy levels of molecule.[14]

$TiO_2$ is a low-cost, non-toxic, high stability and excellent corrosion resistance semiconductor material. Because of the high roughness, the solar radiation can be reflected several time on the surface and absorbed by donor repeatedly, which improve the utilization rate of solar radiation largely. However, the spectral response range of $TiO_2$ is mainly in ultraviolet region and the forbidden band is very broad, which greatly limits the absorption of visible light greatly. But $TiO_2$ can be linked to an acceptor by chemical bond. Ma and co-workers have studied the influence of connection of $TiO_2$ to an acceptor on the properties of solar cells.[15] Their results show that the photoeletric conversion efficiency of solar cell for chemical bond connection is 9 and 60 times than that for weak interaction connection. Under specific conditions, the carotenoid and pheophytin *a* can link to the surface of $TiO_2$ to form a supermolecule, which not only improve the light absorption, but also broaden the spectral response region. Based on this supermolecule, the electrons can directly transfer to the surface or interior of $TiO_2$. It can efficiently increase the charge injection efficiency and even realize the instantaneous charge transfer. Photoinduced electron transfer between a carotenoid and $TiO_2$ nanoparticle has been experimentally reported.[16] Furthermore, self-assembly and photoinduced electron transfer for the system of carotenoid and pheophytin on $TiO_2$ semiconductor surface have also been reported.[17]

In this paper, appropriate bioorganic molecules of carotenoid,

pheophytin *a* and $TiO_2$ have been selected to study the photoinduced charge transfer and energy transfer mechanism, while they are optically excited in electronic transitions. The three-dimensional (3D) visualization technology[18-20] has been adopted to reveal the process of photoinduced charge transfer. Visualizing of the charge transfer process directly demonstrates that the electron transfer from the carotenoid to $TiO_2$ for the carotenoid-pheophytin *a*-$TiO_2$ film in a wider spectroscopy response, which is the key factor to a high efficiency bioorganic (DSSC) solar cell. Further, our results show that method of the chemical bond connection is more suitable for the organic solar cell.

## Calculation methods

The isolated carotenoid,[16] pheophytin *a*,[17] and the complex of carotenoid-pheophytin *a* have been selected as active materials for the bioorganic solar cells. All quantum chemical calculations were performed by Gaussian 09 software.[21] The ground-state geometries were optimized using density functional theory (DFT),[22] B3LYP functional,[23] and 6-31G (d) basis set. The electronic transitions in optical absorption were calculated using the time-dependent DFT (TD-DFT),[24] CAM-B3LYP functional[25] and 6-31G(d) basis set. The vertical excitation energies and oscillation strengths were also calculated at geometries of ground-state. In addition, rutile nanocrystal $TiO_2$ cluster[26] was introduced to build the complex of carotenoid-pheophytin *a*-$TiO_2$, which has been optimized using DFT, B3LYP functional and 6-31G (d) basis set for C, O, N, H, and the LANL2DZ basis set[27] for Ti atom. Charge difference density[18-20] was calculated by three-dimensional (3D) visualization technology to study the relationship between the structure and performance of the carotenoid-pheophytin *a*-$TiO_2$ film. Further, visualization of the molecular system at excited state was realized, which revealed mechanisms of photoinduced charge transfer and energy transfer.

## Results and discussion

The carotenoid (reans-8′-apo-β-caroten-8′-oic acid) and pheophytin *a* are two most common materials in biological nature. Despite strong absorption exists for carotenoid and pheophytin *a*, their spectral responses are limited in a narrow region (420-550 nm). Surprisingly, once they combine to a complex molecule system, the spectral absorption range will be expanded largely.

The carotenoid is a common nature pigment and the molecule structure is shown in Fig.1 (a). The carotenoids mainly absorb blue-violet light and transfer the energy to the pheophytin *a* in photosynthesis. Because of the long conjugate C=C bond, the carotenoid has strong absorption peaks in the visible spectral region. Fig. 1(b) shows the structure of pheophytin *a*, and which consists of tetrapyrrole ring and four methylene groups. In order to broaden the pheophytin *a* spectrum response to the visible light region, the carotenoid molecule was linked to the pheophytin *a* based on coulomb interaction.

The excited states of isolated carotenoid, pheophytin *a* and the complex system of carotenoid-pheophytin *a* have been also calculated (see table 1). Fig. 2(a) shows that a strong absorption peak of the carotenoid, which is located at 456.85 nm, where the oscillator strength reaches to the maximum intensity. In general, oscillator strength can be used to reflect the ability to absorb light as well as the transition probability which reveals that the electric transition of molecules occur in the strong absorption region and thus improve the photoelectric conversion efficiency. Fig. 2(b) shows that the absorption spectra of the pheophytin *a* are mainly located in range from 250 nm to 450 nm. Fifteen excited states have been calculated for the pheophytin *a*, and the oscillator strength of the third and fourth excited state reach to maximum intensities of *f*=0.79 and 1.00, respectively (see table 1). This reveals that the third and fourth excited state have a larger electronic transition probability than other excited states.

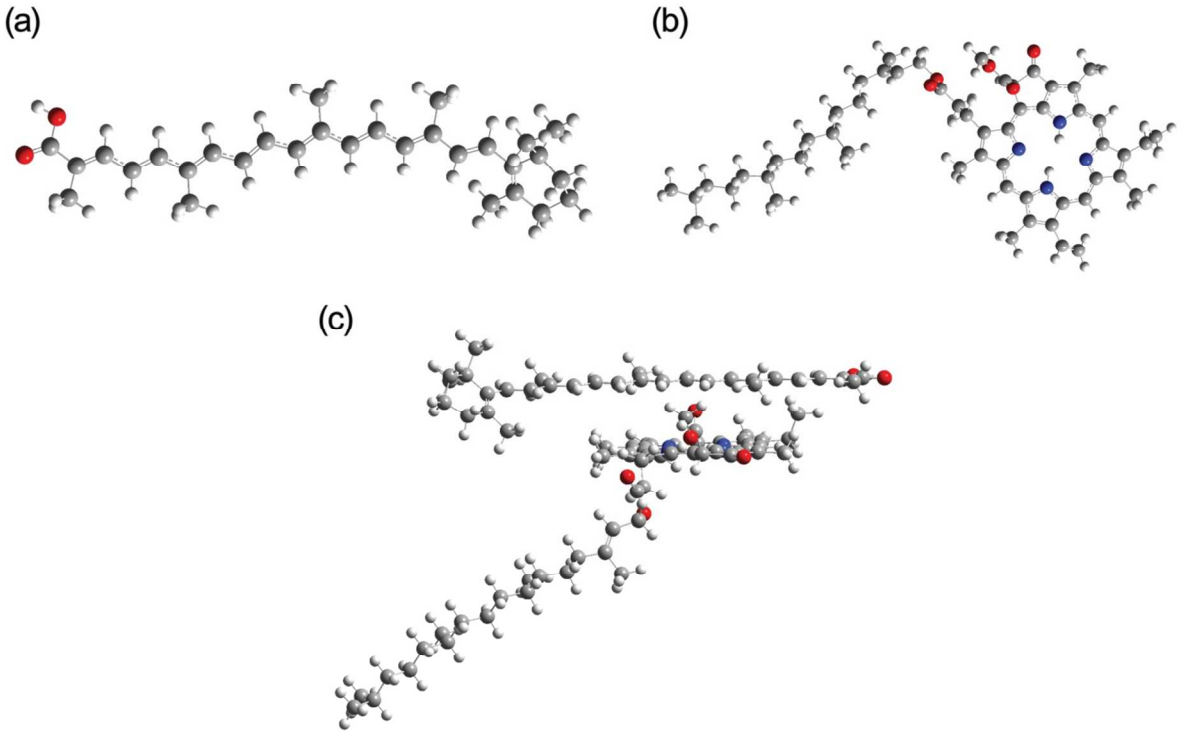


**Fig. 1** The optimized chemical structure. (a) carotenoid, (b) pheophytin *a*, (c) carotenoid -pheophytin *a*.

Furthermore, the pheophytin *a* has a strong absorption, where there is maximum oscillator strength and thus the electronic transition can occur. Fig. 2(c) shows that there are two absorption peaks for the complex of carotenoid-pheophytin *a*. The absorption peak, located at 385.07 nm respectively, arise from the spectral response of the pheophytin *a*, while the peak located at 473.58 nm arises from the spectral response of carotenoid. Interestingly, the spectral response region is largely broadened while the carotenoid and pheophytin *a* are formed to be a complex molecule. The largest oscillator strength in Fig. 2(c) reveals that $S_4$ excited state has strong electron transition ability and light absorption. Based on the above results, the pheophytin *a* and the carotenoid are selected as electron donors in this work.

To better understand the excited-state properties of isolated carotenoid and pheophytin *a*, theory analysis have been performed using the three-dimensional (3D) real space analysis method and the two-dimensional (2D) sit representation. Fig. 3 shows the 3D charge difference densities of carotenoid. Charge difference densities, defined as the difference between the charge density after bonding and the charge density of the corresponding point, is the charge redistribution after the atoms forming a system.[18-20] The direction of the charge transfer in the bonding electron coupling process can be seen clearly. As is shown in Fig. 3, electrons and holes are localized on the spine of carotenoid which reveals that $S_1$, $S_2$ and $S_3$ are localized excited states, and the electrons transfer to the sides of the spine while the holes transfer to the central chains gradually.

**Table 1** Calculated Transition Energies (eV, nm) and Oscillator Strengths (*f*) for the isolated caotenoid and pheophytin a.

| | States | E(ev) [a] | *f* [b] | CI[c] |
|---|---|---|---|---|
| carotenoid | $S_1$ | 2.7139 | 3.5762 | 0.68439(H→L) |
| | $S_2$ | 3.8593 | 0.0793 | 0.67021(H-1→L) |
| | $S_3$ | 4.0016 | 0.0541 | 0.67042(H→L+1) |
| pheophytin *a* | $S_1$ | 2.0943 | 0.0231 | 0.39267(H→L) |
| | $S_2$ | 2.3112 | 0.0027 | 0.37604(H→L) |
| | $S_3$ | 3.2415 | 0.7904 | 0.24173(H→L) |
| | $S_4$ | 3.3997 | 1.0063 | 0.36101(H→L) |
| | $S_5$ | 3.6079 | 0.1600 | 0.61475(H-2→L+1) |
| | $S_6$ | 3.7711 | 0.0117 | 0.51434(H-6→L) |
| | $S_7$ | 3.8336 | 0.3109 | 0.55229(H-2→L) |
| | $S_8$ | 3.9926 | 0.0170 | 0.59530(H-3→L) |
| | $S_9$ | 4.0317 | 0.4418 | 0.44364(H-3→L+1) |
| | $S_{10}$ | 4.1161 | 0.0723 | 0.21271(H-4→L) |
| | $S_{11}$ | 4.2727 | 0.1671 | 0.60836(H→L+2) |
| | $S_{12}$ | 4.3025 | 0.0688 | 0.67389(H-1→L+2) |
| | $S_{13}$ | 4.3699 | 0.0011 | 0.33489(H-8→L+1 |
| | $S_{14}$ | 4.4958 | 0.0009 | 0.38301(H-10→L) |
| | $S_{15}$ | 4.5826 | 0.1316 | 0.64125(H-7→L) |

[a]The numbers in parentheses are the transition energy in wavelength. [b]Oscillator strength. [c]H stands for HOMO and L stands for LUMO, CI coefficients are in absolute values.

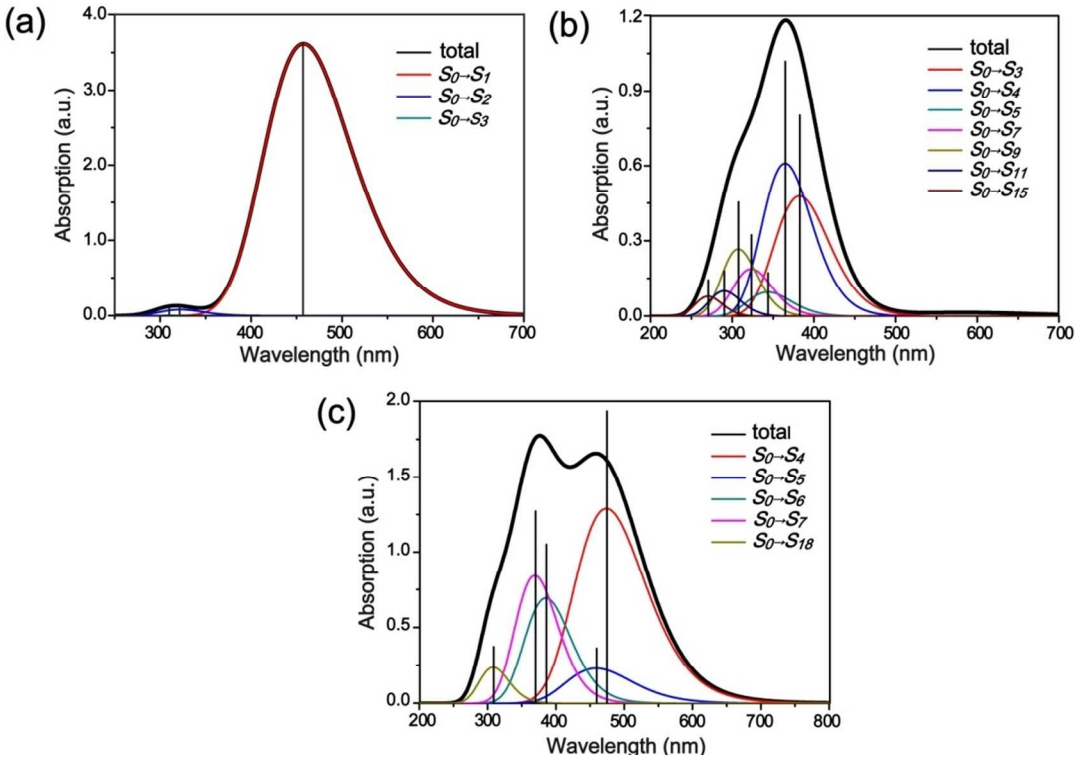


**Fig. 2** The optical electronic state absorption spectra, and (a) carotenoid, (b) pheophytin *a*, (c) carotenoid -pheophytin *a*.

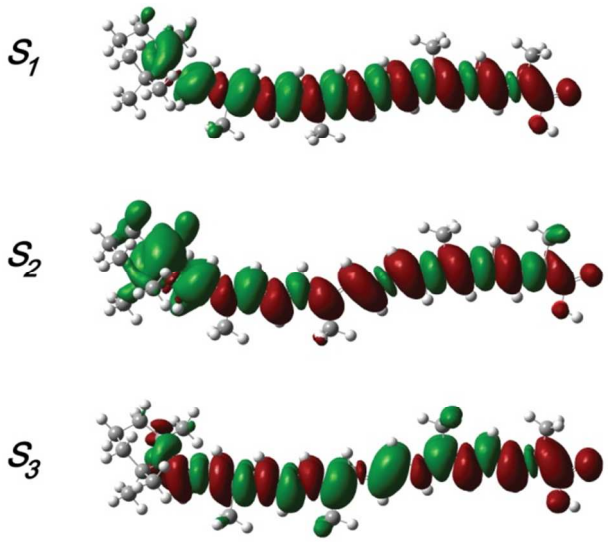


**Fig. 3** Charge difference densities for different electronic excited states of carotenoid, where the green and red stand for the hole and electron, respectively.

The charge difference density of pheophytin *a* is shown in Fig. 4. $S_3$ and $S_4$ are strong absorption located at 382.49 nm and 364.69 nm, respectively. The electrons and holes localized on the whole porphyrin reveal strong charge localization in the pheophytin *a*. $S_{13}$ and $S_{14}$ are weak absorption where electrons and holes are also localized in the whole porphyrin, which further proved the charge localization in pheophytin *a*. Once placing the carotenoid parallel close to the pheophytin *a*, electrons will rapidly transfer between the carotenoid and the pheophytin *a*.

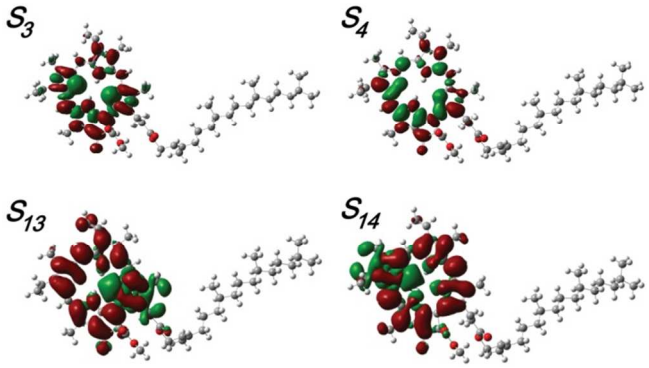


**Fig. 4** Charge difference densities of pheophytin *a*, where the green and red stand for the hole and electron, respectively.

In the transition process of electrons, the binding state is created by the coulomb force between the electrons in the conduction band and the holes in the valence band. The separation of exciton is to generate electrons and holes by overcoming the coulomb force. The Exciton Binding Energy is one of key factors directly determining the separation of electrons and holes in the organic solar cell. The exciton binding energy is mainly from the coulomb force between donor cations and acceptor anions.

**Table 2** Selected electronic transition energies (eV) and the corresponding oscillator strengths (f), main compositions and CI coefficients of carotenoid -pheophytin a.

| States | Transition Energy(eV)[a] | *f*[b] | Δr(Å)[c] | Excited-state Property[d] |
|---|---|---|---|---|
| $S_1$ | 2.0850 (594.65 nm) | 0.0127 | 0.279202 | LE |
| $S_2$ | 2.3051 (537.88 nm) | 0.0036 | 0.426212 | LE |
| $S_3$ | 2.4014 (516.31 nm) | 0.0012 | 4.449655 | ICT |
| $S_4$ | 2.6180 (473.58 nm) | 1.9146 | 2.981704 | ICT |
| $S_5$ | 2.7042 (458.49 nm) | 0.3422 | 4.000988 | ICT |
| $S_6$ | 3.2198 (385.07 nm) | 1.0314 | 0.316830 | ICT |
| $S_7$ | 3.3606 (368.94 nm) | 1.2517 | 0.380151 | ICT |
| $S_8$ | 3.4436 (360.04 nm) | 0.0791 | 4.042327 | ICT |
| $S_9$ | 3.5201 (352.22 nm) | 0.0236 | 4.071160 | ICT |
| $S_{10}$ | 3.5928 (345.09 nm) | 0.1652 | 0.525675 | LE |
| $S_{11}$ | 3.6468 (339.98 nm) | 0.0012 | 4.923839 | ICT |
| $S_{12}$ | 3.7996 (326.31 nm) | 0.0595 | 4.314745 | ICT |
| $S_{13}$ | 3.8029 (326.03 nm) | 0.1976 | 1.611009 | ICT |
| $S_{14}$ | 3.8732 (320.11 nm) | 0.0988 | 3.367877 | ICT |
| $S_{15}$ | 3.9024 (317.72 nm) | 0.0223 | 0.232065 | LE |
| $S_{16}$ | 3.9406 (314.63 nm) | 0.0851 | 4.283794 | ICT |
| $S_{17}$ | 3.9752 (311.89 nm) | 0.0458 | 0.707571 | ICT |
| $S_{18}$ | 4.0259 (307.97 nm) | 0.3523 | 1.388938 | ICT |
| $S_{19}$ | 4.1096 (301.69 nm) | 0.0719 | 3.029693 | ICT |
| $S_{20}$ | 4.2026 (295.02 nm) | 0.1199 | 3.456301 | ICT |

[a] The numbers in parentheses are the transition energy in wavelength.
[b] Oscillator strength. [c]Δr index is a quantitative indicator of electron excitation mode which is a measure of CT length. [d] $PC_{61}BM$ and BT in parentheses present that the density are localized on the fullerene and polymer, respectively.

$$E_{Coul} = \sum_{d \in D, h \in a} \varepsilon \frac{q_d q_a}{\Delta r} \quad (1)$$

where $q_d$ and $q_a$ are the partial charges in atoms d and a from donor cations and acceptor anions, respectively. $\varepsilon$ is the dielectric constant. Δr index is a quantitative indicator of electron excitation mode which is a measure of CT length (see table 2). The value of the exciton binding energy determines whether the separation of electrons and holes is successfully realized. As shown in table 2, the binding energy of carotenoid -pheophytin a reveals that we can get the minimum Δr of 0.279 Å. In this case, the electrons and holes are completely located in pheophytin a where they are hardly to separate and transfer. For the eleventh excited state, Δr reaches to the maximum 4.924 Å. In this case, the electrons are located in pheophytin a and the holes are not completely located in carotenoid. Generally, the separation of electrons and holes is easily realized for a low coulomb force. In other words, the binding energy decreases as increasing Δr and thus increases the separation probability of electrons and holes.

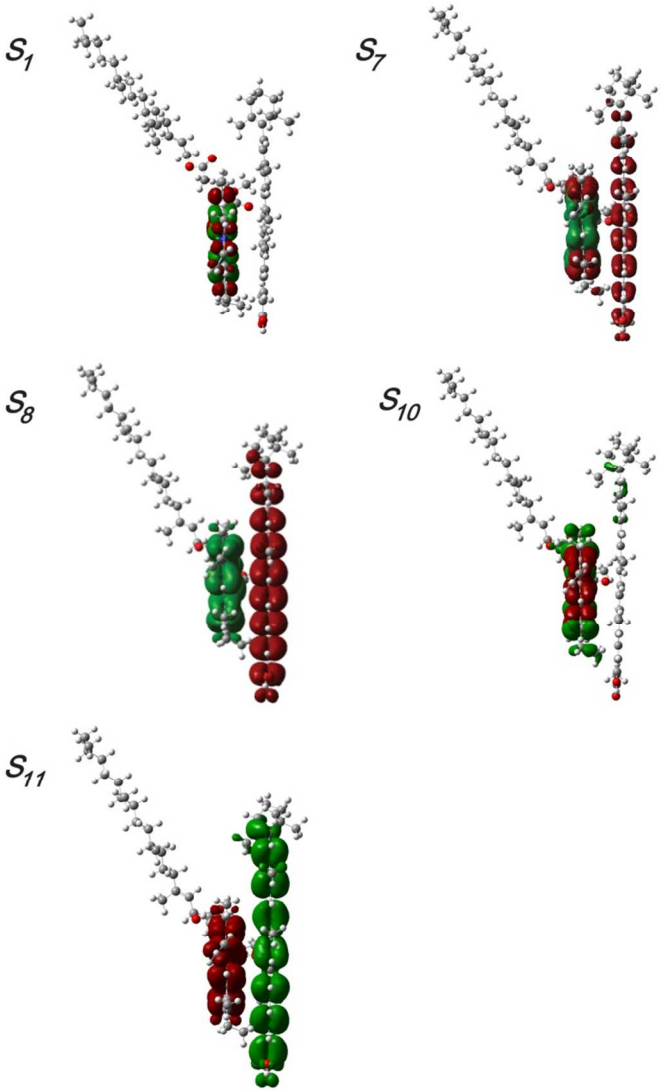


**Fig. 5** Charge difference densities of carotenoid -pheophytin *a*, where the green and red stand for the hole and electron, respectively.

Fig. 5 shows the charge difference density of the complex of carotenoid-pheophytin a. Two kinds of excited states exist in the absorption band of the complex of carotenoid-pheophytin a: one is the strong resonance charge transfer (CT) excited state, where electrons transfer take place from the main chain of cartenoid to the pheophytin a. For the $S_7$, Δr is 0.380 Å, which indirectly reveals a large binding energy, and the electrons are located in both carotenoid and pheophytin a. For the $S_8$, Δr is 4.042 Å, which indirectly reveals a small binding energy where the electrons and holes are easy to separate and then the electrons will completely transfer to cartenoid. The other is the weak resonance charge transfer process, which showed that electrons transfer from the pheophytin a to the main chain of cartenoid. $S_{10}$ is not pure intermolecular charge transfer excited states, since electron and hole are localized on pheophytin a. $S_{11}$ is a pure intermolecular charge transfer excited state, since electron and hole are localized on pheophytin a and carotenoid, respectively.

3D visualization technology can clearly reveal the transfer direction of electric charge in the coupling process of bonding and bonding electrons, but cannot provide the information of electronic coherence and the source of electrons and holes. As a result, the 2D site representation is introduced to analysis the electronic coherence. Note that the larger value along the off-diagonal element in the 2D site representation demonstrates a stronger electronic coherence where reveals a more transfer probability of electric transfer. The diagonal elements reveal a small transfer region of electronic transfer, while those points far away from the diagonal reveal a wider transfer region of electronic transfer. Those points with large value which is close to the diagonal demonstrate a strong electronic coherence between a atom with the adjacent atom.

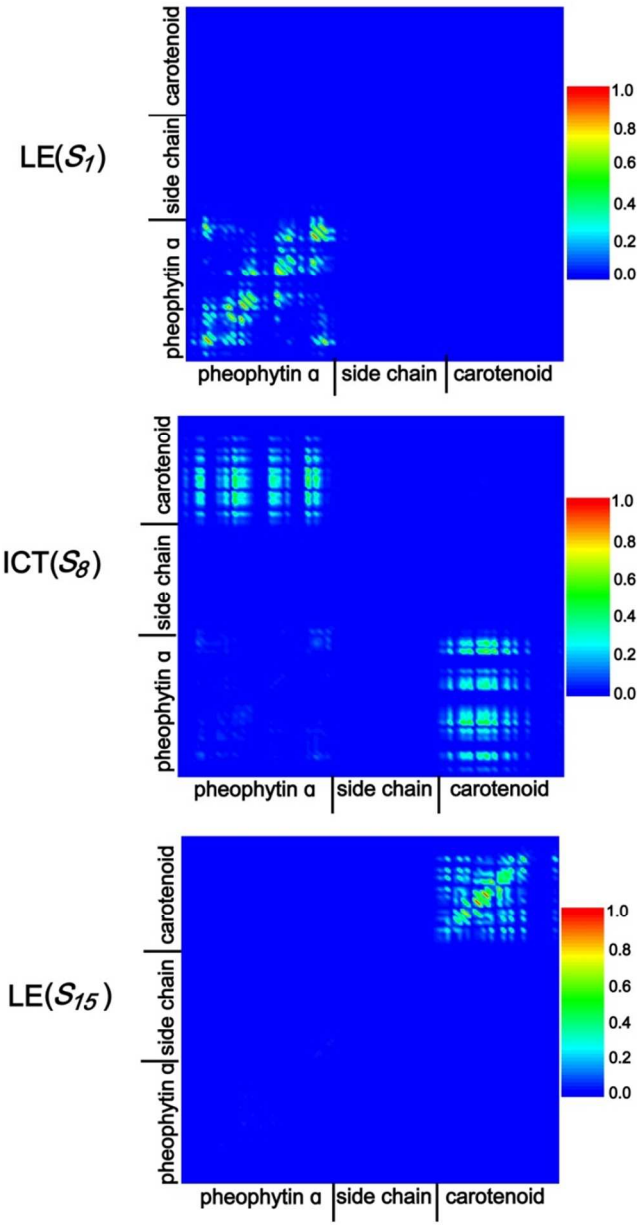


**Fig. 6** The 2D contour plots of the selected transition density matrix of the pheophytin a linked carotenoid with different excite-state properties. The color bars are shown at the right of figure.

As shown in Fig. 6, we observe $S_1$, $S_{15}$ are the localized excited states. For $S_1$, both electron and hole are localized on

pheophytin a molecule and the electron-hole coherence is strong at the left bottom of pheophytin a. For $S_{15}$, both electron and hole are localized on carotenoid molecule. the electron-hole coherence is strong at the top right corner of carotenoid. $S_8$ is a intermolecular electric charge transfer state，where electrons and holes cohere between carotenoid and pheophytin a.

$TiO_2$ has been linked to the complex of carotenoid-pheophytin *a* based on chemical bond and coulomb interaction connections, which were used to study their excited state properties. Simply, the carotenoid-pheophytin *a*-$TiO_2$ has been renamed as C-P-T. Fig. 7(a) shows the connection by coulomb interaction (C-P-T-1), which is π-π connection. The strong absorption peaks ($S_3$, $S_{17}$) are located in the UV-VIS region, and $S_1$, $S_2$, are located in visible region. The strongest oscillator strength is $f$=2.7349 located at 505.58 nm while the weakest oscillator strength is $f$=0.0001 located at 337.63 nm. Fig. 7(b) shows the connection by chemical bond (C-P-T-2). The strong absorption peaks ($S_{11}$, $S_{38}$, $S_{41}$) are located in the UV-VIS region, and $S_1$, $S_2$, $S_3$, $S_4$ are located in visible region. The strongest oscillator strength is $f$=2.7349 located at 506 nm, while the weakest oscillator strength is $f$=0.0001 located at 338 nm. Comparing to Fig. 6(a) and (b), the spectral response range for C-P-T-2 is broader than that for C-P-T-1, where the former is in the range from 300 nm to 750 nm while the latter is in the region between 300 nm and 650 nm.

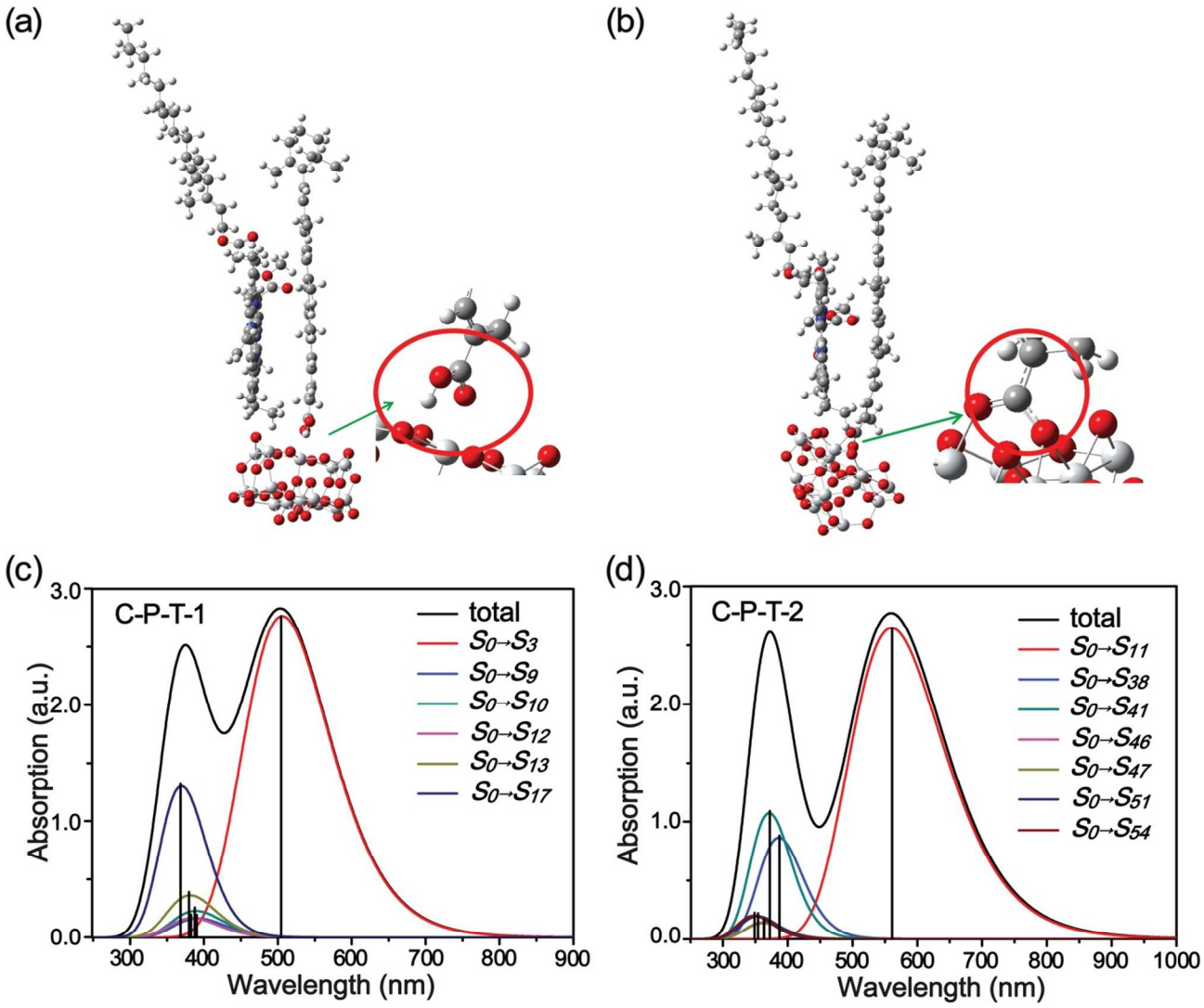


**Fig. 7** The optimized chemical structure and the optical electronic state absorption spectra of carotenoid - pheophytin *a* -$TiO_2$.

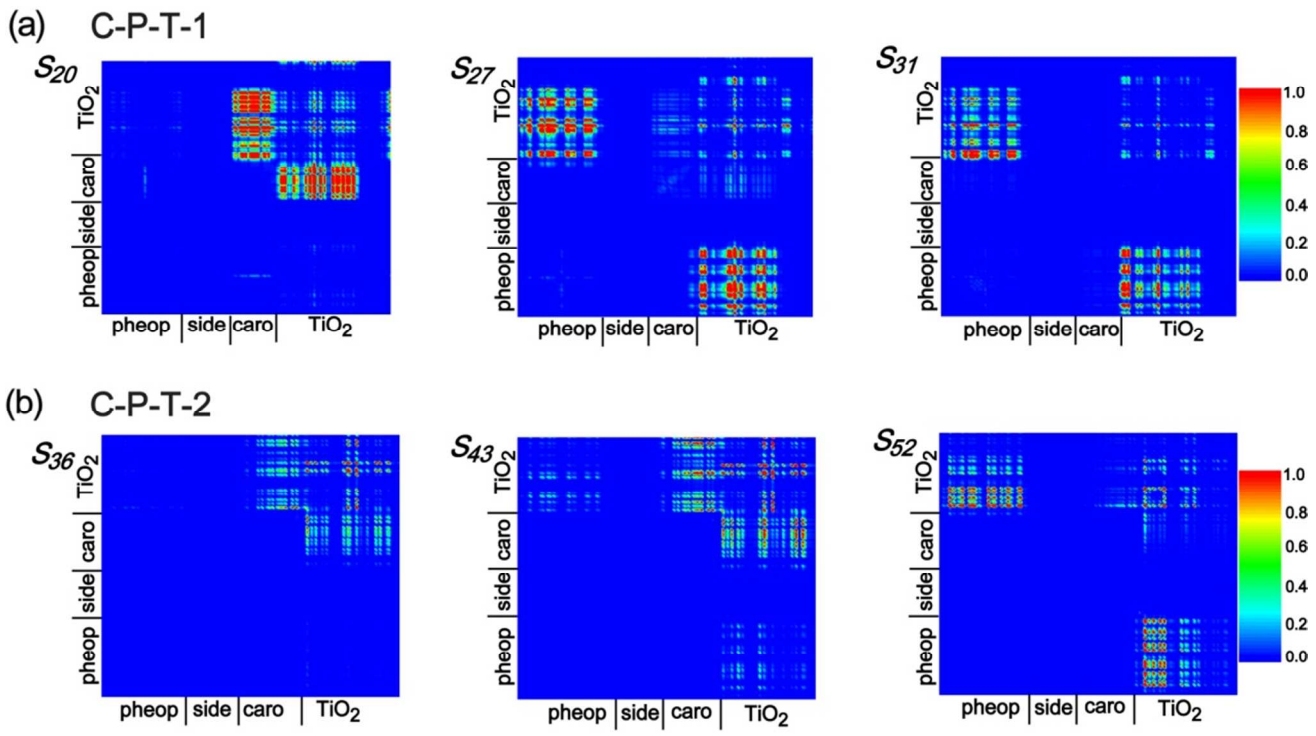


Fig. 8 The 2D contour plots of the selected transition density matrix for C-P-T-1 and C-P-T-2. The color bars are shown at the right of figure.

The study of excited state of carotenoid-pheophytin *a*-$TiO_2$ shows there are three types of charge transfer: one is the electrons transfer from carotenoid to $TiO_2$; the second is the electrons transfer from carotenoid and pheophytin a to $TiO_2$; the last is the electrons transfer form pheophytin a to $TiO_2$. For $S_{20}$, electron and hole are localized in $TiO_2$ and carotenoid where the electron-hole coherence is strong at the crossing of $TiO_2$ and carotenoid, as shown in Fig. 8(a). For $S_{27}$, electrons and holes are localized in $TiO_2$ and carotenoid-pheophytin *a*, respectively where the electron-hole coherence is strong at the crossing of $TiO_2$ and carotenoid-pheophytin *a*. For $S_{31}$, electron and hole are localized on $TiO_2$ and pheophytin *a*, respectively, where the electron-hole coherence is strong at the crossing of $TiO_2$ and pheophytin *a*. As shown in Fig. 8(b), for $S_{36}$, electron and hole are localized in $TiO_2$ and carotenoid, respectively, where the electron-hole coherence is strong at the center of $TiO_2$. For $S_{43}$, electron and hole are localized in $TiO_2$ and carotenoid-pheophytin *a*, respectively, where the electron-hole coherence is strong at the center of $TiO_2$. For $S_{52}$, electron and hole are localized in $TiO_2$ and pheophytin *a*, respectively, where the electron-hole coherence is strong at the left side of $TiO_2$.

Fig. 9 shows the charge difference densities for P-C-T-1 and P-C-T-2. The electric charge transfer for C-P-T-1 in the strong resonance CT excited states occurs between the main chain of cartenoid and $TiO_2$. $S_{13}$ is the pure intermolecule electron transition excited state, where the electrons are localized on the whole $TiO_2$ and the holes are localized on the main chain of cartenoid and pheophytin *a*. However, $S_{10}$ and $S_{12}$ are not pure intermolecular charge transfer excited state, where the electrons transfer from pheophytin *a* to cartenoid, and then to $TiO_2$. Fig. 9 (b) shows that the oscillator strengths of $S_{11}$ ($f$=2.6159) and $S_{41}$ ($f$=1.0594) in C-P-T-2, which are considered as strong absorbing states. In addition, $S_{22}$ and $S_{43}$ are pure intermolecule electronic transfer excited states, because the electronic for the C-P-T-2 is localized. For $S_8$ and $S_{41}$, electrons transfer first from pheophytin *a* to cartenoid, and then to $TiO_2$. $S_{11}$, mainly formed by the electronic transfer from HOMO to LUMO, which is the strongest absorption excited state, which was revealed by the maximum probability of electron transition. By comparing C-P-T-1 with C-P-T-2, the electronic absorption and injection can be directly affected by the way of linking the carotenoid to $TiO_2$. For the chemical bond connection, electrons inject into $TiO_2$ immediately, which can effectively decrease the loss of electrons during the electric charge transfer process. The chemical bond connection can also help for us to improve the light absorption and the photoelectric conversion efficiency.

## Conclusion

In this work, the excited state properties of the isolated carotenoid, pheophytin *a*, the complex of carotenoid-pheophytin *a* and carotenoid-pheophytin *a*-$TiO_2$ film have been studied, using quantum chemical method. The vertical excited energies and absorption spectral have been also investigated. Depending on the three-dimensional visualization technology, visualization of charge transfer can be realized clearly. The complex of carotenoid-pheophytin *a* not only shows a broader spectrum response than the isolated carotenoid and pheophytin *a*, but also demonstrates the strong resonance and weak resonance electric charge separation excited state exists in the absorption band. Visualizing of the charge transfer process directly demonstrates that the electron transfer from the carotenoid to $TiO_2$ for the carotenoid-pheophytin *a*-$TiO_2$ film in a wider spectroscopy

response, which is the key factor to a high efficiency bioorganic solar cell. Chemical bond and coulomb interaction based connections are used to link the carotenoid to $TiO_2$. Further, our results show that the chemical bond connection is more suitable for the organic solar cell.

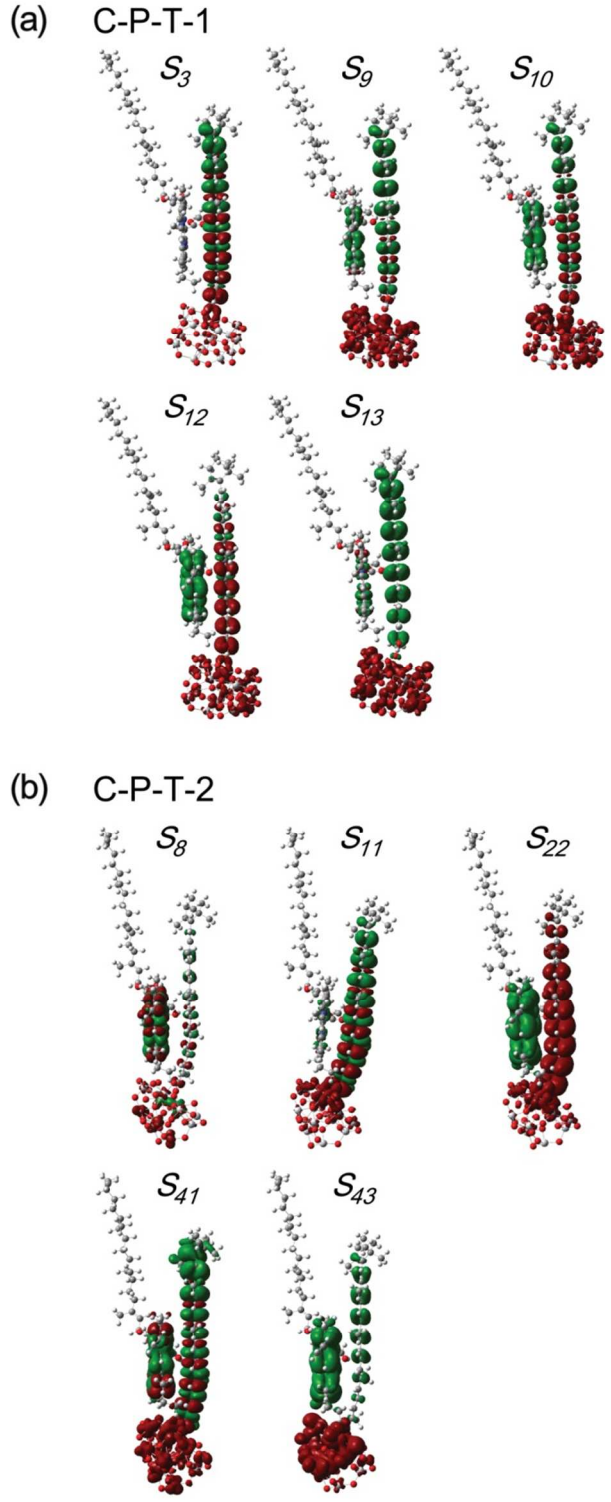


**Fig. 9** Charge difference densities of carotenoid -pheophytin *a*- $TiO_2$, where the green and red stand for the hole and electron, respectively.

## Acknowledgments

This work was supported by National Key Basic Research Program of China (2014CB921001), National Natural Science Foundation (11474141, 91436102, 11374353, 11304135, 11474239 and 21173171), the Special fund based research new technology of methanol conversion and coal instead of oil and the china postdoctoral science Foundation (2014M550158), the Program of Liaoning Key Laboratory of Semiconductor Light Emitting and Photocatalytic Materials, the Scientific Research Foundation for the Returned Overseas Chinese Scholars, State Education Ministry and the Scientific Research Foundation for the Doctor of Liaoning University.

## Notes and references

[a] *Department of Physics, Liaoning University, Shenyang, China. E-mail: yqli@lnu.edu.cn (Y. Q. Li)*
[b] *Institution of Physics, Chinese Academy of Sciences, Beijing, China. E-mail: mtsun@iphy.ac.cn (M. T. Sun); jnchen@iphy.an.cn(J.N. Chen).*
[c] *State Key Laboratory of Molecular Reaction Dynamics, Dalian, China. Institution of Chemical Physics, Chinese Academy of Sciences, Dalian*
[#] *Contributed equally.*

1 R. H. Friend, R. W. Gymer, A. B. Holmes, J. H. Burroughes, R. N. Marks, C. Taliani, D. D. C. Bradley, D. A. D. Santos, J. L. Bredas and M. Logdlund, *Nature*, 1999, **397**, 121.
2 H. E. A. Huitema, G. H. Gelinck, J. B. P. H. Vanderputten, K. E. Kuijk, C. M. Hart, E. Cantatore and D. M. deLeeuw, *Adv. Mater.*, 2002, **14**, 1201.
3 P. Song, Y. Z. Li, F. C. Ma, T. Pullerits and M.T. Sun, *J.Phys. Chem. C,* 2013, **117**, 15879
4 C. J. Brabec, N. S. Sariciftci and J. C. Hummelen, *Adv. Funct. Mater.,* 2001, **11**, 15.
5 Q. Zhou and T. M. Swager, *J. Am. Chem. Soc.*, 1995, **117**, 12593.
6 G. Yu, J. Gao, J. C. Hummelen, F. Wudl and A.J. Heeger, *Seience,* 1995, **270**, 1789.
7 S. Mukamel, S. Tretiak, T. Wagersreiter and V. Chernyak, *Science.* 1997, **277**, 781; S. Tretiak and S. Mukamel, *Chem. Rev.*, 2002, **102**, 3171.
8 S. Tretiak, A. Saxena, R. L. Martin and A. R. Bishop, *Phys. Rev. Lett.,* 2002, **89**, 097402; S. Tretiak, A. Saxena, R. L. Martin and A.R. Bishop, *Proc. Natl. Acad. Sci*., 2003, **99**,2185.
9 M. Chegaar, N. Nehaoua and A. Bouhemadou, *Energy Convers Manage*, 2008, **49**, 1376.
10 J. Chandrasekaran, D. Nithyaprakash, K. B. Ajjan, S. Maruthamuthu, D. Manoharan and S.Kumar, *Renewable Sustainable Energy Rev*, 2011, **15**, 1228.
11 K. Bouzidi, M. Chegaar and M. Aillerie, *Energy Procedia*, 2012, **18**, 1601.
12 S. E. Shaheen, C.J. Brabec, N.S. Sariciftci, F. Padinger, T. Fromherz and J. C. Hummelen. *Appl. Phys. Lett.*, 2001, **78**, 841.
13 B. Regan, M. Grätzel, Nature, 1991, 353, 737.
14 S. L. Wu, H. P. Lu, H. T. Yu, S. H. Chuang, C.L. Chiu, C. W. Lee, E. W. G. Diau and C. Y. Yeh, *Energy. Environ. Sci.*, 2010, **3**, 949.
15 T. Ma, K. Inoue, H. Noma, K.Yao and E. Abe, *J. Photochem. Photobiol. Chem.*, 2002, **152**, 207.
16 J. Pan, G. Benko, Y. H. Xu, T. Pascher, L. C. Sun, V. Sundstrom and T. Polı´vka, *J. Am.Chem Soc.*, 2002, **124**, 13949.
17 J. X. Pan, Y. H. Xu, L. C. Sun, V. Sundstrom, T. Polivka, *J. Am. Chem. Soc.* 2004, 126, 3066.
18 M. T. Sun, *J. Chem. Phys.,* 2007, **127**, 084706
19 Y. Li, T. Pullerits, M. Zhao and M. Sun, *J. Phys. Chem. C,* 2011, **115**. 21865.
20 L. Xia, M. Chen, X. Zhao, Z. Zhang, J. Xia, H. Xu, M. Sun, *J. Raman Spectrosco.* 2014, 45, 533.
21 M. J. Frisch, G. W. Trucks, H. B. Schlegel, G. E. Scuseria, M. A. Robb, J. R.. Cheeseman, G. Scalmani, V. Barone, B. Mennucci, G. A. Petersson, et al. Gaussian 09, Revision A. 02; Gaussian, Inc.: Wallingford, CT, 2009.

22 P. Hohenberg and W. Kohn, *Phys. Rev.*, 1964, **136**, 864.
23 C. Lee, W. Yang and R. G. Parr, *Phys. Rev.*, 1988, **37**, 785.
24 E. K. U. Gross and W. Kohn, *Phys. Rev. Lett.*, 1985, **55**, 2850.
25 T. Yanai, D. Tew and N. Handy, Chem. *Phys. Lett*., 2004, **393**, 51.
26 Z.W. Qu, G.J. Kroes, *J. Phys. Chem. C*, 2007, 111, 16808.
27 Hay, P. J.; Wadt, W. R. *J. Chem. Phys.* 1985, 82, 270.